Membrane-Based Affinity Purification to Identify Target Proteins of a Small-Molecule Drug

Liu Yang,[a] Loan Bui,[b] Donny Hanjaya-Putra,[b,c] and Merlin L. Bruening*,[a,c]

[a]Department of Chemistry and Biochemistry, [b]Department of Aerospace and Mechanical Engineering, Bioengineering Graduate Program, and [c]Department of Chemical and Biomolecular Engineering, University of Notre Dame, Notre Dame, Indiana 46556, United States

Corresponding author: Merlin L. Bruening E-mail: mbruenin@nd.edu

ABSTRACT: Identifying the target proteins of small-molecule drug candidates is important for determining their molecular mechanisms of action. Porous membranes derivatized with such small molecules may provide an attractive target-identification platform due to a high protein-capture efficiency during flow through membrane pores. This work employs carbonic anhydrase II (CAII) binding to immobilized 4-(2-aminoethyl)benzenesulfonamide (AEBSA) to examine the efficiency and selectivity of affinity capture in modified membranes. Selective elution of captured protein, tryptic digestion, tandem mass spectrometry analysis, and label-free quantification (LFQ) identify CAII as the dominant AEBSA target in diluted serum or cell lysate. CAII identification relies on determining the ratio of protein LFQ intensities in sample and control experiments, where free AEBSA added to the control loading solution limits CAII capture. Global proteomics shows that the spiked CAII is the only protein with a $\log_2$ ratio consistently >2, and the detection limit for CAII identification is 0.004 wt% of the total protein in 1:4 diluted human serum or 0.024 wt% of the total protein from breast cancer cell lysates. The same approach also identifies native CAII in human kidney cell lysate as an AEBSA target. Comparison of affinity capture using membranes, Affi-Gel 10 resin or M-270 Dynabeads derivatized with AEBSA suggests that only membranes allow identification of low-abundance CAII as a target.

This work explores the use of porous affinity membranes for identifying the protein targets of a small-molecule drug. During flow of serum or cell lysates through modified membranes, immobilized drugs capture target proteins. Subsequent mass spectrometry (MS) analysis identifies the eluted targets through comparison with control experiments. Such target identification is crucial for understanding the mechanisms of action of potential drugs identified through phenotypic screening, and for predicting side effects due to drug interactions with off-target proteins.[1]

Phenotypic screening identifies small-molecule drugs that modulate the properties of cells or organisms. This method is more likely to produce active drugs than target-based screening because the small molecule "hits" already show cellular activity.[2] However, subsequent identification of target proteins is a bottleneck for phenotype-based drug development.[3-4] Thus, many recent studies modified potential small-molecule drugs so that they tag or modify target proteins to enable their identification.[5-9]

Despite recent progress in tagging methods, the relatively simple technique of affinity purification remains an effective approach to identify protein targets of small-molecule drugs.[4, 10] This strategy typically consists of five steps: 1) immobilization of a small molecule on a substrate; 2) capture of target proteins from a protein mixture; 3) rinsing to remove nonspecifically adsorbed proteins; 4) elution; and 5) identification and quantitation of eluted proteins using sodium dodecyl sulfate polyacrylamide gel electrophoresis (SDS-PAGE) and/or MS.[4] This method has identified targets of small-molecule drugs such as tacrolimus,[11] imatinib,[12] and vancomycin.[13] Moreover, quantitative MS-based proteomics analyses effectively distinguish specific targets from nonspecific binding in affinity purification.[14-15]

Although often successful in target identification, affinity purification has two main drawbacks. First, it requires small molecules with functional groups that enable immobilization without altering biological activity. Thus, other methods employ changes in protein properties (e.g. melting temperature shift,[16] solubility in an organic solvent,[17] resistance to oxidation,[18] or proteolysis[19]) to identify protein targets without the need for a coupling point on the small molecule. However, the properties of some proteins will not greatly change upon binding a small molecule.[20-21] The need for an appropriate moiety to immobilize a small molecule of interest is sometimes only a minor limitation. Studies of structure-activity relationships are integral to the development of small-molecule drugs and show whether a specific functional group can participate in immobilization without altering activity. Additionally, some drug libraries contain specific groups for immobilizing the molecules.[22-23]

A second challenge in affinity purification is that nonspecifically adsorbed proteins may suppress signals from target proteins or produce false-positive identifications.[24] To overcome this, affinity purification often examines differences in levels of target proteins in sample and control experiments. The two main types of control experiments include binding to substrates without immobilized small molecules or capture with the free small molecule added to the loading solution to compete for

binding sites on the targets.[20] After digestion of captured proteins, subsequent quantitative comparison of peptide signals in sample and control experiments allows statistical determination of potential targets. However, even with such controls nonspecific adsorption remains a challenge in affinity purification. For example, control substrates typically do not show the same nonspecific adsorption properties as substrates derivatized with the small molecule.[25] Moreover, if nonspecific adsorption is extensive in both control and sample experiments, it will both mask signals of real targets and give false-positive identifications.[26]

The overall success of target identification using affinity purification depends on both efficient capture of target proteins and low nonspecific adsorption. We hypothesize that affinity purification using vertical flow through membranes with immobilized small molecules could enhance protein capture and decrease nonspecific adsorption relative to bead-based capture. Flow through μm-sized membrane pores rapidly brings target proteins to binding sites to avoid diffusion limitations on binding.[27] Additionally, rapid flow limits residence times and enhances rinsing, which may decrease nonspecific adsorption. Finally, the use of membranes modified with poly(acrylic acid) (PAA)-containing films enables extensive small-molecule immobilization and protein binding with low nonspecific adsorption at physiological ionic strength.[28]

To examine membrane-based target identification, we employ carbonic anhydrase II (CAII) binding to an inhibitor, 4-(2-aminoethyl)benzenesulfonamide (AEBSA), as a model system. AEBSA has a primary amine group that allows covalent immobilization to PAA-containing membranes, and the structure-activity relationship of CAII binding to AEBSA is well studied.[29] Prior studies show that CAII is amenable to affinity purification with benzensulfonamides.[6, 30] **Scheme 1** shows the protocol for these studies in which CAII in human serum or cell lysate binds to immobilized AEBSA during passage through a derivatized membrane. Subsequent rinsing, elution and digestion of bound protein, and LC-MS/MS analysis with label-free quantitative proteomics enable comparison of binding with (control experiment) and without (sample experiment) free AEBSA in the serum or lysate. In the control, free AEBSA should bind to target proteins in solution to limit their binding to the membrane and decrease their signal intensities in eluate analyses.

This paper explores membrane-based methods for target identification and includes optimization of immobilized ligand density, development of selective elution, investigation of detection limits for target identification in serum and cell lysates, and native CAII capture in human kidney lysate. To investigate whether membranes can enhance affinity purification relative to other substrates, this study compares CAII identification using membranes, agarose beads (Affi-Gel 10)[6, 31] or magnetic beads (Dynabeads M-270 Carboxylic Acid)[32] derivatized with AEBSA.

EXPERIMENTAL SECTION

Materials. Hydroxylated nylon membranes (LoProdyne LP, 1.2 μm pore size, 100 μm thick) were obtained from Pall. Poly(acrylic acid) (PAA) was acquired from Sigma-Aldrich (molecular weight (Mw) ≈ 100,000 Da, 35% aqueous solution) or Polysciences (Mw ≈ 120,000 Da, 35% aqueous solution). Polyethylenimine (PEI, branched, Mw = 25,000 Da), bovine carbonic anhydrase II (CAII), 4-(2-aminoethyl)benzenesulfonamide (AEBSA), 1-ethyl-3-(3-dimethylaminopropyl)carbodiimide hydrochloride (EDC), N-hydroxysuccinimide (NHS), and

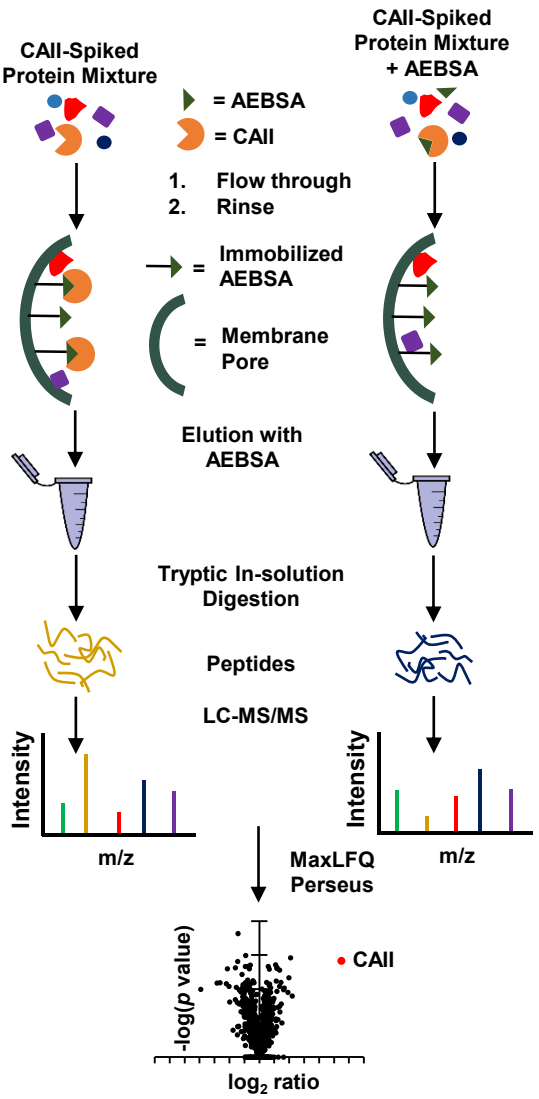

Scheme 1. Workflow for identifying CAII as a target of AEBSA. Sample (CAII-spiked protein mixture, left) and control (CAII-spiked protein mixture with free AEBSA, right) solutions pass through membranes containing immobilized AEBSA. Subsequent LC-MS/MS analysis of eluted and digested proteins leads to plots of $\log_2$ ratios of protein LFQ intensities in the sample and control analyses along with *p* values. Abbreviations: CAII - carbonic anhydrase II; AEBSA - 4-(2-aminoethyl)benzenesulfonamide; MaxLFQ - MaxQuant label-free quantification.

human serum were used as received from Sigma-Aldrich. Human kidney whole tissue lysate in buffer was purchased from Novus Biologicals. **Section S1** of the supporting information describes the buffer for kidney lysate and detailed procedures for breast cancer cell lysate protein extraction. Buffers were prepared using analytical grade chemicals and deionized water (Milli-Q, 18.2 MΩ). The buffer (pH 7.4) compositions were: binding buffer - 20 mM phosphate buffer in 150 mM NaCl; washing buffer I - 20 mM phosphate buffer in 500 mM NaCl; and washing buffer II - 20 mM phosphate buffer in 500 mM NaCl with 0.1% Tween-20.

Immobilization of AEBSA in Porous Nylon Membranes. Membranes were modified with PAA/PEI/PAA films, and reacted with AEBSA using EDC/NHS chemistry as described in **Section S1** of the supporting information.

Capture of CAII from Diluted Human Serum or Cell Lysate. Varying amounts of CAII were spiked into breast cancer cell lysate or binding buffer-diluted human serum. Kidney tissue lysate was diluted with binding buffer to give 2.0 mg/mL of total protein. A protein mixture (0.25 mL) was passed through an AEBSA-modified membrane (1-cm diameter) followed by washing the membrane with 5 mL of binding buffer and 5 mL of washing buffer I. (Washing entails passing the solutions through the membrane.) Further washing included 5 mL of washing buffer II and 5 mL of deionized water for membranes loaded with ≥0.01 mg/mL spiked CAII, or only 5 mL of deionized water (no washing buffer II) for membranes loaded with <0.01 mg/mL spiked CAII or kidney tissue lysate. (Loading and washing employed a flow rate of 0.5 mL/min.) In subsequent elution, 0.5 mL of 2.0 mg/mL AEBSA flowed through the membranes at ~0.1 mL/min. Eluates were concentrated to ~40 μL using a 10kDa cutoff filter (Amicon Ultra) and then were loaded on 4-20% gradient SDS-PAGE gels or dried down for digestion and LC-MS/MS analysis.

Mass Spectrometry Analysis of Eluates from AEBSA-Modified Membranes. Dried eluates were digested in solution and then desalted using ZipTips. (See **Section S1** of the supporting information for the protein-digestion procedure.) The digests were dried using a SpeedVac and reconstituted with 15 μL of 0.1% formic acid. Two μL of the reconstituted solution was injected into a Waters NanoAcquity UPLC system coupled to a Q Exactive Hybrid Quadrupole-Orbitrap mass spectrometer (Thermo Fisher) to identify proteins in eluates. UPLC employed a BEH C18 column (Waters, 100 μm × 100 μm, 300 Å, 1.7 μm). Peptide separation used a method with a 60-minute gradient from 4 to 33% B with a flow rate of 900 nL/min. (Solution A was 0.1% formic acid in LC-MS grade H_2O, and solution B was 0.1% formic acid in acetonitrile.) Full MS scans were acquired from 415 to 2000 m/z at a resolution of 70,000, and the top 12 precursors were selected for fragmentation. MS/MS scanned from 200 to 2000 m/z at a resolution of 17,500 with an AGC target of 2×10^5. Each sample was analyzed in triplicate for label-free quantification analysis.

MS/MS Data Processing. Raw LC-MS/MS files were processed by MaxQuant (version 1.6.12.0) and were searched against the human serum proteome (790 proteins) or the Uniprot human proteome UP000005640 (74,788 Proteins) with the addition of trypsin and bovine CAII sequences. In MaxQuant, the main search peptide mass tolerance was 4.5 ppm, and the product ion mass tolerance was set to 20 ppm. Trypsin was set as the enzyme with a maximum of two missed cleavages. Variable modifications included oxidation (M), acetyl (protein N-term), deamidation (NQ), Gln→pyro-Glu, and Glu→pyro Glu. The fixed modification was carbamidomethyl on cysteine. The "match between runs" was checked with default settings. LFQ analysis was selected to get LFQ intensities. For peptide quantification, modifications included oxidation (M), acetyl (protein N-term) and deamidation (NQ), and the "discard unmodified counterpart peptides" was unchecked. LFQ intensities were uploaded to Perseus (version 1.6.12.0) to generate volcano plots with a $\log_2$ ratio of sample and control LFQ intensities against a –log (*p* value).

RESULTS AND DISCUSSION

This section develops membrane-based affinity capture to identify targets of AEBSA. We first examine the effect of AEBSA immobilization density on protein binding and then establish selective elution methods to collect target proteins from membranes loaded using protein mixtures with and without spiked CAII. Subsequent studies show that analyses of digested eluates (via LC-MS/MS with LFQ) differentiate specific and nonspecific binding in both human serum and cell lysates. Finally, we compare target identification using affinity capture with membranes or resins (Affi-Gel 10 and Dynabeads M-270).

Protein Binding as a Function of Ligand (AEBSA) Density. As **Section S2** of the supporting information shows, studies with films on flat surfaces suggest that there is an optimal AEBSA immobilization density for capturing large amounts of CAII while maintaining low nonspecific adsorption. Thus, we varied the AEBSA concentration used for membrane derivatization to control the extent of AEBSA immobilization and optimize protein binding. The supporting information shows that the amount of AEBSA immobilization increases approximately linearly with the AEBSA concentration in the derivatization solution (**Figure S5**). For AEBSA-modified membranes loaded with CAII-spiked diluted serum, SDS-PAGE analyses of eluted protein suggest that derivatization with 0.5 mg/mL AEBSA gives lower nonspecific adsorption than derivatization with higher AEBSA concentrations (**Figure S6**). Thus, all further experiments employed circulation of 2 mL of 0.5 mg/mL AEBSA for ligand immobilization in a 2-cm diameter membrane.

Ideally, modified membranes should capture all of the target protein from solution. Breakthrough curves (**Figure S7**) show that AEBSA-derivatized membranes adsorb around 90% of the CAII during passage of the first 2 mL of ~0.1 mg/mL CAII (in binding buffer) through the membrane. Thus, to ensure a high binding efficiency, subsequent capture experiments passed only 1 mL of CAII solution through a 2-cm diameter membrane or 0.25 mL of CAII solution through a 1-cm diameter membrane. The high CAII binding from the first mL of solution is consistent with isothermal titration calorimetry data that give a dissociation constant, K_d, of 5.21 ± 0.95 μM for the CAII-AEBSA complex in solution (**Figure S8**). A literature study reports a similar K_d value.[33] Presuming that the immobilized AEBSA has the K_d value for CAII, binding of all of the protein from a 1 mL solution would require <55% of the equilibrium binding capacity (see **Section S4** in the supporting information).

Development of Selective Elution Methods. In addition to protein capture, identification of drug targets requires effective methods for selective target elution from membranes. In studies of elution, we first loaded membranes with 1 mL of 0.05 mg/mL CAII in 1:4 binding buffer-diluted human serum. Under these conditions, CAII is 0.4 wt% of the total protein. After sequentially passing binding buffer and washing buffers I and II through the loaded membrane, we eluted bound proteins with either 2% SDS in 100 mM dithiothreitol (DTT) or 2.0 mg/mL AEBSA in deionized water. The SDS/DTT mixture is a stringent eluent that denatures proteins and dissociates ligand-target complexes.[34] As the electrophoretic gel in **Figure S9A** shows, the SDS/DTT solution elutes a large amount of nonspecifically adsorbed protein in addition to the CAII target. Such nonspecifically bound proteins may suppress the MS signal of target proteins and lead to false-positive target identifications.

In contrast to SDS/DTT elution, free AEBSA in solution should compete with immobilized ligand to *specifically* elute protein targets. In **Figure S9B**, the five consecutive free-AEBSA eluates from a CAII-loaded membrane each display a dominant CAII band (**lanes 6-10**). This occurs even though CAII is only 0.4 wt% of the total protein. Chromatographic

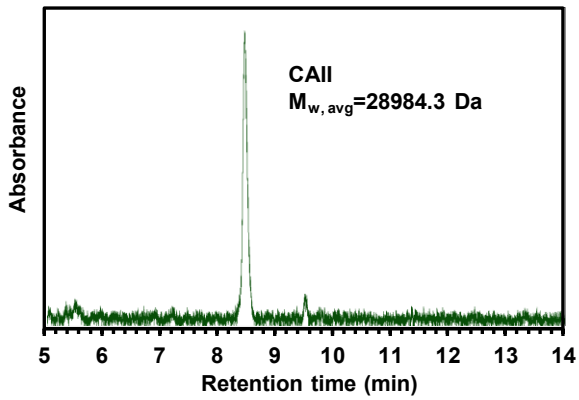

Figure 1. Chromatogram (UV detection) of proteins eluted from an AEBSA-modified membrane loaded with CAII (0.4 wt% of total protein) in 1:4 diluted human serum. Elution used free AEBSA. The small peak around 9.6 min is not a protein (there is no charge envelope in the MS analysis at 9.6 min).

analysis of the eluate yields a dominant peak at 8.6 min corresponding to a species with Mw = 28984.3 Da (**Figure 1**). Thus, the eluate contains remarkably pure CAII. Although the CAII recovery with the free AEBSA eluent is not as high as with SDS/DTT (compare **Figures S9A and S9B**), selective elution simplifies the eluted protein composition and avoids the need for surfactant removal prior to protein digestion for MS-based analysis. For these reasons, the following studies employ solutions of free AEBSA as the eluent.

Control Experiments to Differentiate Specific and Nonspecific Binding. When CAII is 0.4 wt% of the total protein in spiked human serum, after capture and specific elution from the membranes, CAII provides the darkest band in SDS-PAGE (**Figure S9B)** and the highest absorbance in a chromatogram (**Figure 1**). Thus, one might distinguish this target from other proteins simply based on its high signal intensity. However, this identification strategy is not statistically definitive, and it is not effective for low-abundance targets. As the fraction of CAII in protein mixtures decreases, the amount of nonspecifically adsorbed (and subsequently eluted) proteins will eventually exceed the amount of CAII.

Most target-identification methods compare the abundance of eluted proteins in sample and control experiments to differentiate between specific and nonspecific adsorption.[35] The control experiments often employ capture from a protein solution containing the free drug, which binds to the target protein in solution to decrease its specific adsorption.[15, 36] Following this strategy, we compare protein adsorption from diluted human serum with and without the addition of free AEBSA. To limit variations due to small differences in modification of different membranes, parallel sample and control experiments employ two pieces (1-cm diameter) taken from the same AEBSA-modified membrane (2-cm diameter).

The electrophoretic gel in **Figure 2** compares sample and control experiments for binding of 0.05 mg/mL CAII (0.4 wt% of total protein) in 1:4 human serum diluted in binding buffer. After capture in a membrane and washing, the protein eluted from the membrane (in the absence of free AEBSA) shows a dominant band for CAII (**lane 5**). In contrast, the eluate from the control experiment (binding in the presence of free AEBSA) shows no noticeable protein bands (**lane 10**). Quantitation of the differences in the band intensities between multiple sample and control experiments could statistically identify potential

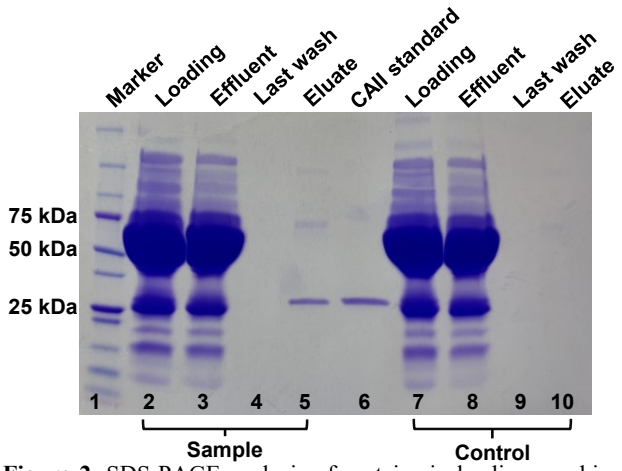

Figure 2. SDS-PAGE analysis of proteins in loading, washing, and elution aliquots from sample and control experiments. Lane 1: molecular weight ladder; lanes 2-5 are from the sample experiment and lanes 7-10 are from the control experiment. Lanes 2-3: loading solution (0.05 mg/mL CAII spiked in 1:4 binding buffer-diluted human serum) before and after passing through the membrane, respectively. Lane 4: last wash. Lane 5: eluate from the sample experiment (15 µL out of 40 µL of total eluate). Lane 6: CAII standard (1.0 µg). Lanes 7 and 8: loading solution (0.05 mg/mL CAII spiked in 1:4 human serum in binding buffer containing 2.0 mg/mL AEBSA) before and after passing through the membrane, respectively. Lane 9: last wash. Lane 10: eluate from the control experiment.

protein targets.[37] However, most target identification studies employ mass spectrometry for quantification.

Label-Free Quantification of Proteins from Sample and Control Experiments. Quantitation of differences in peptide and protein intensities in different samples often employs differential labeling approaches, such as stable isotope labeling by amino acids in cell culture[15] or the introduction of isobaric tags.[26] Such methods exhibit quantitative accuracy and a wide dynamic range.[38] However, time-consuming and expensive sample-preparation procedures complicate these approaches and may limit the number of sample replicates.[39] Label-free quantification (LFQ) is convenient[40] and allows examination of more replicates, although it may show lower accuracy than the labelling approaches. Advanced mass spectrometers and bioinformatics software have improved the performance of proteomics experiments[41-42] and catalyzed the development of LFQ.[43]

MaxLFQ is a generic LFQ approach integrated in MaxQuant software,[44] and this technique requires minimal but parallel analyses.[45] In this work the parallel analyses result from nanoUPLC with MS/MS detection for digested proteins from sample and control experiments. Using Perseus, we processed the MaxLFQ data to obtain the $\log_2$ ratios of protein LFQ intensities in sample and control experiments along with p values for whether the differences between control and sample LFQ values are significant for three replicate analyses (**Scheme 1**).

Figure 3 shows a volcano plot for proteins eluted from an AEBSA-modified membrane previously loaded with 0.001 mg/mL CAII-spiked diluted serum. In the control experiment, free AEBSA in the loading solution should inhibit target binding during passage through the membrane. Thus, proteins whose MaxLFQ intensities decrease significantly in the control experiment are the most likely targets. Importantly with CAII concentrations ranging from 0.001 to 0.05 mg/mL in diluted human serum, CAII is the only protein that reproducibly shows a

$\log_2$ ratio >2 (**Figure 3** and **Figure S10**). We repeated all of these experiments with two different membranes and obtained

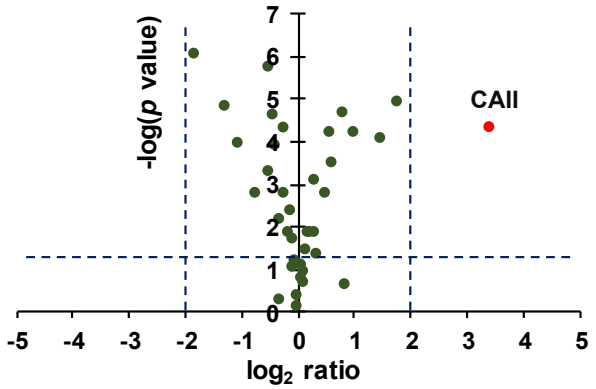

Figure 3. Volcano plot of the ratio of eluate LFQ intensities in sample (no free AEBSA) and control (free AEBSA in the loading solution) experiments. The y-axis shows the –log(*p*) values for a t-test of whether the sample and control experiments differ significantly. The loading solutions contained 0.001 mg/mL (0.008 wt%) CAII spiked into 1:4 human serum in binding buffer, and the wt% is relative to the total protein. The plot shows 37 total proteins.

similar results (**Figure S11** in **Section S6** of the supporting information shows data for other replicates).

With 0.0005 mg/mL CAII (~0.004 wt% of total protein), one experiment shows that CAII is still the only protein with a $\log_2$ ratio >2 in a volcano plot (**Figure S12**). However, another replicate exhibits CAII LFQ intensity in the sample but not in the control experiment. This prevents statistical identification of CAII as a target. Nevertheless, CAII is the only protein that shows a significant intensity in the sample and no intensity in the control experiment so one might think it is a target. When the spiked CAII concentration is 0.0001 mg/mL (0.0008 wt% of total protein), neither sample nor control experiment shows an LFQ intensity for CAII. Thus, the detection limit for identifying CAII as a target in serum is ~0.004 wt% of total protein. This detection limit is about 5-fold lower than the literature value of ~0.02 wt% CAII when using a DNA-programmed affinity labelling method.[7] Low detection limits are important for identifying low-abundance targets.

In addition to looking for proteins that consistently show a $\log_2$ ratio >2, we also determined proteins that have a $\log_2$ ratio >1 and a *p* value <0.05 in multiple volcano plots. These proteins may bind to AEBSA with weak affinity. Considering ten volcano plots obtained with different concentrations of spiked CAII in serum, seven other proteins show a $\log_2$ ratio >1 and a *p* value <0.05 in at least three experimental replicates (**Table S1**). However, only hemopexin, insulin-like growth factor-binding protein, and histidine-rich glycoprotein (HRG) exhibit a $\log_2$ ratio >1 in more than four volcano plots. These three proteins may weakly adsorb to AEBSA. HRG gives a $\log_2$ ratio >1 only in volcano plots where the concentrations of spiked CAII are relatively high (≥ 0.0025 mg/mL). Thus, HRG may interact with CAII rather than AEBSA. Hemopexin and insulin-like growth factor-binding protein show $\log_2$ ratios >1 even with low CAII concentrations in some cases.

Human serum is a biased protein mixture as ~50 wt% of the total protein is albumin.[46] Moreover, 10 proteins account for 90 wt% of the total human serum protein, and the other 10 wt% primarily consists of 12 dominant species.[46] Thus, we also examined CAII capture from breast cancer cell lysates (MDA-MB-231) to explore membrane-based affinity purification with a larger number of detectable proteins. Breast cancer cell lysates contain ~8,000 different detectable proteins with a wide range of molecular weights and reported abundances.[47] Similar to the work in serum, we spiked different amounts of CAII into cell lysates to establish the limit of detection for this protein. **Figure S13** shows the SDS-PAGE analysis of loading and eluate solutions for a protein mixture consisting of 0.01 mg/mL CAII spiked into a cell lysate containing 2.1 mg/mL of total protein. As the stained gel shows, the cell lysate clearly has a higher variety of abundant proteins than human serum (compare **lane 2** in **Figure S9B** to **lane 3** in **Figure S13**). Nevertheless, the eluate from the sample experiment presents only one light band (~29 kDa**, lane 6**, **Figure S13**), and no such band is visible in the control experiment (**lane 10, Figure S13**), suggesting specific capture from cell lysate and elution of CAII from the AEBSA-modified membranes.

Figure 4 shows a volcano plot of proteins eluted from PAA/PEI/PAA-AEBSA-derivatized membranes previously loaded with CAII-spiked MDA-MB-231 cell lysate. Compared to experiments with human serum, eluates from cell lysates contain more proteins because of the increased complexity of the protein mixture. Even with the cell lysate, CAII is still the only protein (out of 436 total proteins with determinable $\log_2$ ratios) that shows a $\log_2$ ratio substantially >2 when the spiked CAII concentration is 0.0025 mg/mL (0.12 wt%, **Figure 4**). This is also the case with a CAII concentration of 0.01 mg/mL (0.48 wt%, **Figure S14**). We repeated these experiments with two different membranes and obtained similar results although three other proteins show $\log_2$ ratios just greater than 2 (**Figure S15** in the supporting information shows data for other replicates).

In the case of cell lysate spiked with 0.0005 mg/mL CAII (0.024 wt% of total protein), the average CAII $\log_2$ ratio is 3.12 in four replicate experiments. However, this ratio is >2 only in two of the replicates (**Figure S16**). Permutation-based false discovery rate calculations indicate that the CAII $\log_2$ ratios are significant in all four replicates. In two additional experimental replicates, CAII shows signals only in the sample but not in control experiments. A number of other proteins also show significant $\log_2$ ratios (see below).

With 0.0001 mg/mL CAII (0.005 wt% of total protein) in MDA-MB-231 cell lysate, a LFQ intensity for CAII appears only in the sample experiment. However, other proteins also show signals in the sample but not the control experiments.

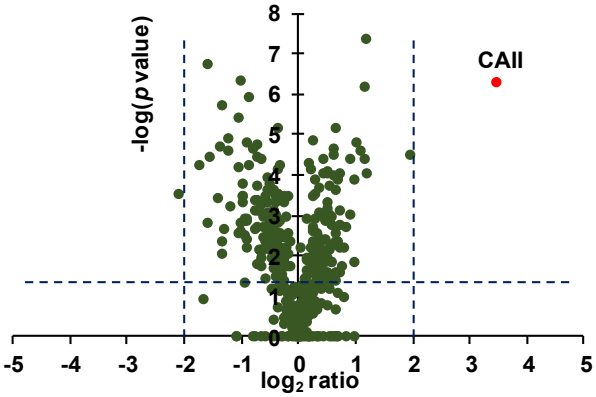

Figure 4. Volcano plot of the ratio of eluate LFQ intensities in sample (no free AEBSA) and control (free AEBSA in the loading solution) experiments. The loading solutions contained 2.1 mg/mL cell lysate spiked with CAII at a concentration of 0.0025 mg/mL (0.12 wt% of total protein). The plot shows 436 total proteins.

Similar to results with diluted serum, when the CAII concentration is below ~0.0005 mg/mL, we cannot identify this protein as a possible drug target. However, with more concentrated cell lysates, the wt% at which we can identify drug targets may decrease. In the case of 0.0005 mg/mL CAII in the solution, we inject only 60 fmoles of this protein into the mass spectrometer for analysis (assuming a 10% recovery). At higher total protein concentrations, for a given CAII wt% we could inject more CAII in the instrument and possibly achieve identification at lower abundance. Additionally, for high-affinity targets one could pass more solution through the membrane to obtain increased target capture.

As in the study of proteins captured from human serum, we also looked for proteins that show a $\log_2$ ratio >1 and a *p* value <0.05 in multiple volcano plots for breast cancer cell lysate. **Table S2** lists all proteins that exhibit a $\log_2$ ratio >1 in at least three out of ten volcano plots. Of particular note, adenylosuccinate lyase (ADSL) has a $\log_2$ ratio >1 in five volcano plots, and its average $\log_2$ ratio in all plots is 1.02. One might wonder why we do not see human carbonic anhydrase proteins in the cell lysate. In related MCF-7 cells, human carbonic anhydrase II ranks 5,789th among proteins in terms of abundance,[47] so we are unlikely to detect it.

To demonstrate target identification with native CAII, we investigated protein capture from human kidney tissue lysate, which contains CAII in relatively high abundance (~0.2 wt% of total protein).[48] **Figure S17** shows the SDS-PAGE analysis of loading and eluate solutions when loading a membrane with 2.0 mg/mL of kidney lysate protein. A light band at ~29 kDa is present in the eluate from the sample **(lane 5**) but not in the control experiment (**lane 10**), suggesting specific capture from kidney lysate and elution of CAII. In contrast, bands located at ~40 kDa and ~250 kDa are likely nonspecifically bound proteins because they are present in both sample and control experiments.

Figure 5 shows a volcano plot of proteins eluted from PAA/PEI/PAA-AEBSA-derivatized membranes previously loaded with kidney tissue lysates. CAII clearly shows the highest $\log_2$ ratio (out of 220 total proteins with determinable $\log_2$ ratios). In two additional replicates with different membranes (**Figure S18**), CAII also gives the highest $\log_2$ ratio. **Table S3** lists all proteins that exhibit a $\log_2$ ratio >1 in at least two out of three experiments. In particular, pyruvate dehydrogenase E1 component subunit beta and 2-oxoisovalerate dehydrogenase subunit alpha are potential targets of AEBSA. We identified

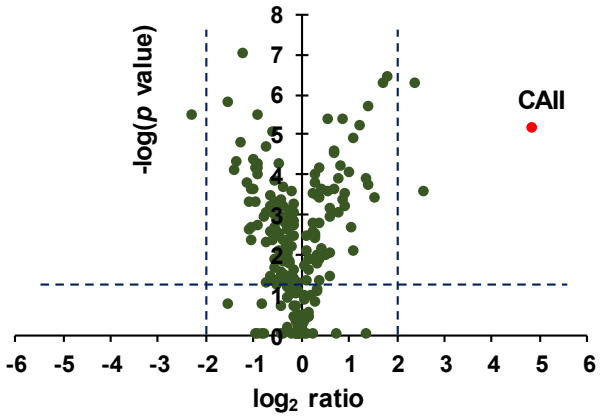

Figure 5. Volcano plot of the ratio of eluate LFQ intensities in sample (no free AEBSA) and control (free AEBSA in the loading solution) experiments. The loading solutions contained 2.0 mg/mL kidney tissue lysate. The plot shows 220 proteins.

these proteins despite their reported low abundance (0.01 wt% - 0.05 wt%).[49]

Comparison of Modified Membranes and Beads for Target Identification. This section compares CAII affinity capture and target identification using membranes, agarose beads (Affi-Gel 10), and magnetic beads (Dynabeads M-270 Carboxylic Acid). Such comparisons are difficult because the performance of a given method depends greatly on specific conditions and experience.[50] Nevertheless, to make the comparison as fair as we could in a reasonable time frame, we followed manufacturer protocols (**Section S1**) and attempted to optimize the amount of AEBSA immobilization for target identification with the two different beads. **Section S8** in the supporting information describes our selection of conditions for CAII capture with different methods.

Affi-Gel 10 is an agarose gel with a 10-carbon spacer arm whose end contains an N-hydroxysuccinimide ester group that readily reacts with a primary amino group in a ligand to form an amide bond. These beads are attractive because their hydrophilic surfaces minimize nonspecific adsorption.[4] The 10-atom spacer arm reduces steric hindrance to target binding, and Affi-Gel 10 has a protein-binding capacity as high as 35 mg per mL of resin.[51] However, the gel slurry is viscous[52] and utilizing exactly the same amount of gel in sample and control experiments is challenging. Additionally, gels stick to vial walls and stirring is difficult. Nevertheless, when modified with AEBSA, these gels effectively capture CAII (see below).

M-270 Carboxylic Acid Dynabeads are uniform magnetic beads covered by a hydrophilic layer of glycidyl ether and carboxylic acid groups. After activation with EDC/NHS, we coupled AEBSA to these substrates. Use of a magnet to attract the Dynabeads to the side of a microcentrifuge tube conveniently separates beads from washing and elution solutions. Moreover, downstream analysis of captured targets could employ either conventional elution or direct on-bead digestion of proteins.

When using Affi-Gel 10 for CAII capture from serum prior to protein elution and LC-MS/MS analysis, CAII has the highest or second-highest LFQ intensity of all eluted proteins when its loading concentration is high (0.05 mg/mL, 0.4 wt% of total protein). In fact, CAII peptide signals in the digested eluate account for around 50% of the total peptide LFQ intensity, whereas in membrane-based affinity capture this value is around 30% with the same loading solution. Moreover, compared to membrane methods the Affi-Gel 10 gives about 40% fewer proteins with measurable $\log_2$ ratios, suggesting less nonspecific adsorption. However, Affi-Gel 10 shows an intense CAII signal in both sample and control experiments, which results in a $\log_2$ ratio of only around 2 as **Figure S19** shows. Evidently free AEBSA does not effectively prevent binding to the Affi-Gel 10 in the control. In a single experiment with a spiked-CAII concentration of 0.01 mg/mL and capture on derivatized Affi-Gel 10, LFQ CAII intensities show a $\log_2$ ratio <0.5 (**Figure S20A)**.

The relatively high CAII LFQ intensities in control experiments with Affi-Gel 10 might stem from the large volume of gel and, hence, the large amount of immobilized AEBSA employed in these experiments (see **Table S4**). We can decrease the amount of immobilized AEBSA by lowering the concentration of AEBSA in the solution used to modify Affi-Gel. Lowering the amount of immobilized AEBSA from 0.50 mg to 0.13 mg did not affect the results (compare **Figure S19** to **Figure S20B**). Further decreasing the amount of AEBSA immobiliza-

tion to 0.05 mg results in very low CAII LFQ intensity in sample and control experiments. In addition, the use of smaller agarose volumes is difficult due to the challenge of pipetting these beads. If available, larger lysate volumes might improve these analyses, as literature studies use a larger ratio of lysate to gel volume.[15, 32] For agarose, an alternative control experiment might also compare gel with and without AEBSA immobilization.[53] However, nonspecific adsorption to Affi-Gel modified with a small molecule such as ethanolamine may be very different than nonspecific adsorption to Affi-Gel modified with AEBSA. Thus, we prefer the control experiment with free AEBSA in solution.

Dynabeads are attractive for simple sample handling. However, even with a high amount of spiked CAII (0.05 mg/mL) in diluted serum, after capture on Dynabeads we did not detect CAII in the proteins eluted with free AEBSA. In an effort to increase protein detection using Dynabeads, we digested the captured proteins directly on the beads. In this case, even with 0.05 mg/mL CAII in serum, CAII gives only the 5th most abundant LFQ intensity of captured proteins digested on beads. In addition to CAII, kininogen-1 and histidine-rich glycoprotein also show significant fold changes between sample and control experiments (**Figure S21**). With 0.01 mg/mL CAII spiked into 1:4 diluted human serum, the CAII signal in sample experiments with on-bead digestion was low and not present in all analytical replicates. These results are consistent with a lower AEBSA immobilization capacity on Dynabeads compared to membranes and Affi-Gel 10. In principle, one could employ a higher bead volume to increase protein-binding, but experiments with larger bead volumes are expensive due to the high cost of these materials. Thus, we used the amounts of Dynabeads mentioned in previous studies.[53-54]

In summary, in our hands immobilization of AEBSA on Affi-Gel 10 allows identification of CAII as a target only at the highest CAII concentrations (0.05 mg/mL) in serum, and the $\log_2$ ratio is only 2. With on-bead digestion, Dynabeads may identify CAII as a target only when it is present at high concentrations (0.05 mg/mL) in serum. In contrast, membranes identify CAII as a target at concentrations as low as 0.0005 mg/mL in serum, and CAII typically shows the highest $\log_2$ ratio of any protein. Moreover, the membranes are easier to work with than Affi-Gel because the gel slurry is viscous, which makes reproducible sample handling difficult.

CONCLUSIONS

Porous membranes derivatized with AEBSA selectively and efficiently capture CAII from diluted serum or cell lysate. Moreover, comparison of protein LFQ intensities in sample and control experiments clearly differentiates CAII from nonspecifically adsorbed proteins at CAII abundances as low as 0.004 wt% of total protein. Convective flow through PAA-containing membrane pores allows rapid binding and limits nonspecific adsorptions. Moreover, the high density of –COOH groups should allow immobilization of a wide range of amine-containing small-molecule drugs.[27, 55] However, the modified membranes are not yet commercial products, and the membrane technique requires apparatuses that are not common in many labs. Relative to capture using Affi-Gel 10 and Dynabeads, in our hands affinity purification with membranes enables CAII identification at 100-fold lower concentrations. Nevertheless, the analysis is not sufficient for detecting target proteins at abundances <40 ppm. Future work with increased protein loading or a higher elution efficiency should further lower detection limits.

ASSOCIATED CONTENT

Supporting Information

The supporting information is available free of charge on the ACS Publication website at DOI:XXX.
Experimental details, reflectance FTIR studies of AEBSA immobilization and CAII adsorption on thin films, breakthrough curves for CAII binding in AEBSA-modified membranes, SDS-PAGE analysis of proteins eluted by SDS/DTT or free AEBSA, additional replicate volcano plots for CAII capture from human serum or cell lysates, tables of other potential protein targets, discussion of ligand immobilization conditions for Affi-Gel 10 and Dynabeads, and volcano plots for protein capture with Affi-Gel 10 and Dynabeads (PDF)

AUTHOR INFORMATION

Corresponding Author

Email: mbruenin@nd.edu; Phone: (574) 631-3024

ORCID

Merlin L. Bruening: 0000-0002-4553-5143

Notes

The authors declare no competing financial interest.

ACKNOWLEDGEMENTS

We gratefully acknowledge funding of this work by the U.S. National Science Foundation through grant 1903967. We thank Dr. Matthew M. Champion from the University of Notre Dame for helpful discussions. We also thank Dr. William Boggess and Dr. Mijoon Lee from the Notre Dame Mass Spectrometry & Proteomics Facility for help with sample analysis.

REFERENCES

(1) Xie, L.; Xie, L.; Bourne, P. E. Structure-based systems biology for analyzing off-target binding. *Curr. Opin. Struc. Biol.* **2011,** *21* (2), 189-199.
(2) Lee, J. A.; Berg, E. L. Neoclassic drug discovery: the case for lead generation using phenotypic and functional approaches. *J. Biomol. Screen.* **2013,** *18* (10), 1143-1155.
(3) Schenone, M.; Dancik, V.; Wagner, B. K.; Clemons, P. A. Target identification and mechanism of action in chemical biology and drug discovery. *Nat. Chem. Biol.* **2013,** *9* (4), 232-240.
(4) Kawatani, M.; Osada, H. Affinity-based target identification for bioactive small molecules. *MedChemComm* **2014,** *5* (3), 277-287.
(5) Tulloch, L. B.; Menzies, S. K.; Fraser, A. L.; Gould, E. R.; King, E. F.; Zacharova, M. K.; Florence, G. J.; Smith, T. K. Photo-affinity labelling and biochemical analyses identify the target of trypanocidal simplified natural product analogues. *PLOS Negl. Trop. Dis.* **2017,** *11* (9), e0005886.
(6) Mabuchi, M.; Shimizu, T.; Haramura, M.; Tanaka, A. Identification and purification of target protein using affinity resin bearing a photo-labile linker. *Bioorg. Med. Chem. Lett.* **2015,** *25* (16), 3373-3377.
(7) Li, G.; Liu, Y.; Liu, Y.; Chen, L.; Wu, S. Y.; Liu, Y.; Li, X. Y. Photoaffinity labeling of small-molecule-binding proteins by DNA-templated chemistry. *Angew. Chem. Int. Edit.* **2013,** *52* (36), 9544-9549.
(8) Hill, Z. B.; Pollock, S. B.; Zhuang, M.; Wells, J. A. Direct proximity tagging of small molecule protein targets using an engineered NEDD8 ligase. *J. Am. Chem. Soc.* **2016,** *138* (40), 13123-13126.
(9) Herner, A.; Marjanovic, J.; Lewandowski, T. M.; Marin, V.; Patterson, M.; Miesbauer, L.; Ready, D.; Williams, J.; Vasudevan, A.; Lin, Q. 2-aryl-5-carboxytetrazole as a new photoaffinity label for drug target identification. *J. Am. Chem. Soc.* **2016,** *138* (44), 14609-14615.

(10) Tulloch, L. B.; Menzies, S. K.; Coron, R. P.; Roberts, M. D.; Florence, G. J.; Smith, T. K. Direct and indirect approaches to identify drug modes of action. *IUBMB LIFE* **2018,** *70* (1), 9-22.
(11) Liu, J.; Farmer, J. D.; Lane, W. S.; Friedman, J.; Weissman, I.; Schreiber, S. L. Calcineurin is a common target of cyclophilin-cyclosporine A and FKBP-FK506 complexes. *Cell* **1991,** *66* (4), 807-815.
(12) He, G.; Luo, W. J.; Li, P.; Remmers, C.; Netzer, W. J.; Hendrick, J.; Bettayeb, K.; Flajolet, M.; Gorelick, F.; Wennogle, L. P.; Greengard, P. Gamma-secretase activating protein is a therapeutic target for alzheimer's disease. *Nature* **2010,** *467* (7311), 95-98.
(13) Koteva, K.; Hong, H. J.; Wang, X. D.; Nazi, I.; Hughes, D.; Naldrett, M. J.; Buttner, M. J.; Wright, G. D. A vancomycin photoprobe identifies the histidine kinase VanSsc as a vancomycin receptor. *Nat. Chem. Biol.* **2010,** *6* (5), 327-329.
(14) Blagoev, B.; Kratchmarova, I.; Ong, S. E.; Nielsen, M.; Foster, L. J.; Mann, M. A proteomics strategy to elucidate functional protein-protein interactions applied to EGF signaling. *Nat. Biotechnol.* **2003,** *21* (3), 315-318.
(15) Ong, S. E.; Schenone, M.; Margolin, A. A.; Li, X.; Do, K.; Doud, M. K.; Mani, D. R.; Kuai, L.; Wang, X.; Wood, J. L.; Tolliday, N. J.; Koehler, A. N.; Marcaurelle, L. A.; Golub, T. R.; Gould, R. J.; Schreiber, S. L.; Carr, S. A. Identifying the proteins to which small-molecule probes and drugs bind in cells. *Proc. Natl. Acad. Sci. U.S.A.* **2009,** *106* (12), 4617-4622.
(16) Ball, K. A.; Webb, K. J.; Coleman, S. J.; Cozzolino, K. A.; Jacobsen, J.; Jones, K. R.; Stowell, M. H. B.; Old, W. M. An isothermal shift assay for proteome scale drug-target identification. *Commun. Biol.* **2020,** *3* (1), 75.
(17) Zhang, X.; Wang, Q.; Li, Y.; Ruan, C.; Wang, S.; Hu, L.; Ye, M. Solvent-induced protein precipitation for drug target discovery on the proteomic scale. *Anal. Chem.* **2020,** *92* (1), 1363-1371.
(18) West, G. M.; Tucker, C. L.; Xu, T.; Park, S. K.; Han, X.; Yates, J. R., 3rd; Fitzgerald, M. C. Quantitative proteomics approach for identifying protein-drug interactions in complex mixtures using protein stability measurements. *Proc. Natl. Acad. Sci. U.S.A.* **2010,** *107* (20), 9078-9082.
(19) Hwang, H. Y.; Kim, T. Y.; Szász, M. A.; Dome, B.; Malm, J.; Marko-Varga, G.; Kwon, H. A.-O. X. Profiling the protein targets of unmodified bio-active molecules with drug affinity responsive target stability and liquid chromatography/tandem mass spectrometry. *Proteomics* **2020,** *20* (9), 1900325.
(20) Jung, H. J.; Kwon, H. J. Target deconvolution of bioactive small molecules: the heart of chemical biology and drug discovery. *Arch. Pharm. Res.* **2015,** *38* (9), 1627-1641.
(21) Lomenick, B.; Hao, R.; Jonai, N.; Chin, R. M.; Aghajan, M.; Warburton, S.; Wang, J.; Wu, R. P.; Gomez, F.; Loo, J. A.; Wohlschlegel, J. A.; Vondriska, T. M.; Pelletier, J.; Herschman, H. R.; Clardy, J.; Clarke, C. F.; Huang, J. Target identification using drug affinity responsive target stability (DARTS). *Proc. Natl. Acad. Sci. U.S.A.* **2009,** *106* (51), 21984-21989.
(22) Khersonsky, S. M.; Jung, D.-W.; Kang, T.-W.; Walsh, D. P.; Moon, H.-S.; Jo, H.; Jacobson, E. M.; Shetty, V.; Neubert, T. A.; Chang, Y.-T. Facilitated forward chemical genetics using a tagged triazine library and zebrafish embryo screening. *J. Am. Chem. Soc.* **2003,** *125* (39), 11804-11805.
(23) Kim, Y. K.; Chang, Y. T. Tagged library approach facilitates forward chemical genetics. *Mol. Biosyst.* **2007,** *3* (6), 392-397.
(24) Ziegler, S.; Pries, V.; Hedberg, C.; Waldmann, H. Target identification for small bioactive molecules: finding the needle in the haystack. *Angew. Chem. Int. Edit.* **2013,** *52* (10), 2744-2792.
(25) Tashiro, E.; Imoto, M. Target identification of bioactive compounds. *Bioorg. Med. Chem.* **2012,** *20* (6), 1910-1921.
(26) Wang, J.; Gao, L.; Lee, Y. M.; Kalesh, K. A.; Ong, Y. S.; Lim, J.; Jee, J. E.; Sun, H.; Lee, S. S.; Hua, Z. C.; Lin, Q. Target identification of natural and traditional medicines with quantitative chemical proteomics approaches. *Pharmacol. Ther.* **2016,** *162*, 10-22.
(27) Dong, J.; Bruening, M. L. Functionalizing microporous membranes for protein purification and protein digestion. *Annu. Rev. Anal. Chem.* **2015,** *8*, 81-100.
(28) Dai, J. H.; Baker, G. L.; Bruening, M. L. Use of porous membranes modified with polyelectrolyte multilayers as substrates for protein arrays with low nonspecific adsorption. *Anal. Chem.* **2006,** *78* (1), 135-140.
(29) Nocentini, A.; Vullo, D.; Bartolucci, G.; Supuran, C. T. N-Nitrosulfonamides: A new chemotype for carbonic anhydrase inhibition. *Bioorgan. Med. Chem.* **2016,** *24* (16), 3612-3617.
(30) Chen, G.; Heim, A.; Riether, D.; Yee, D.; Milgrom, Y.; Gawinowicz, M. A.; Sames, D. Reactivity of functional groups on the protein surface: development of epoxide probes for protein labeling. *J. Am. Chem. Soc.* **2003,** *125* (27), 8130-8133.
(31) Chen, X. P.; Zhao, C. Y.; Li, X. L.; Wang, T.; Li, Y. Z.; Cao, C.; Ding, Y. H.; Dong, M. Q.; Finci, L.; Wang, J. H.; Li, X. Y.; Liu, L. Terazosin activates PGK1 and HSP90 to promote stress resistance. *Nat. Chem. Biol.* **2015,** *11* (1), 19-25.
(32) Ito, T.; Ando, H.; Suzuki, T.; Ogura, T.; Hotta, K.; Imamura, Y.; Yamaguchi, Y.; Handa, H. Identification of a primary target of thalidomide teratogenicity. *Science* **2010,** *327* (5971), 1345-1350.
(33) Roy, B. C.; Banerjee, A. L.; Swanson, M.; Jia, X. G.; Haldar, M. K.; Mallik, S.; Srivastava, D. K. Two-prong inhibitors for human carbonic anhydrase II. *J. Am. Chem. Soc.* **2004,** *126* (41), 13206-13207.
(34) Mabuchi, M.; Haramura, M.; Shimizu, T.; Nishizaki, T.; Tanaka, A. Selective elution of target protein from affinity resins by a simple reductant with a thiol group. *Bioorg. Med. Chem. Lett.* **2010,** *20* (24), 7361-7364.
(35) Yamamoto, K.; Yamazaki, A.; Takeuchi, M.; Tanaka, A. A versatile method of identifying specific binding proteins on affinity resins. *Anal. Biochem.* **2006,** *352* (1), 15-23.
(36) Bantscheff, M.; Eberhard, D.; Abraham, Y.; Bastuck, S.; Boesche, M.; Hobson, S.; Mathieson, T.; Perrin, J.; Raida, M.; Rau, C.; Reader, V.; Sweetman, G.; Bauer, A.; Bouwmeester, T.; Hopf, C.; Kruse, U.; Neubauer, G.; Ramsden, N.; Rick, J.; Kuster, B.; Drewes, G. Quantitative chemical proteomics reveals mechanisms of action of clinical ABL kinase inhibitors. *Nat. Biotechnol.* **2007,** *25* (9), 1035-1044.
(37) Issaq, H.; Veenstra, T. Two-dimensional polyacrylamide gel electrophoresis (2D-PAGE): advances and perspectives. *Biotechniques* **2008,** *44* (5), 697-700.
(38) Chen, X.; Wei, S.; Ji, Y.; Guo, X.; Yang, F. Quantitative proteomics using SILAC: principles, applications, and developments. *Proteomics* **2015,** *15* (18), 3175-3192.
(39) Nukala, S. B.; Baron, G.; Aldini, G.; Carini, M.; D'Amato, A. Mass spectrometry-based label-free quantitative proteomics to study the effect of 3PO drug at cellular level. *ACS Med. Chem. Lett.* **2019,** *10* (4), 577-583.
(40) Millikin, R. J.; Solntsev, S. K.; Shortreed, M. R.; Smith, L. M. Ultrafast peptide label-free quantification with flashLFQ. *J. Proteome Res.* **2018,** *17* (1), 386-391.
(41) Trujillo, E. A.; Hebert, A. S.; Brademan, D. R.; Coon, J. J. Maximizing tandem mass spectrometry acquisition rates for shotgun proteomics. *Anal. Chem.* **2019,** *91* (20), 12625-12629.
(42) Riley, N. M.; Hebert, A. S.; Coon, J. J. Proteomics moves into the fast lane. *Cell. Syst.* **2016,** *2* (3), 142-143.
(43) Ramus, C.; Hovasse, A.; Marcellin, M.; Hesse, A. M.; Mouton-Barbosa, E.; Bouyssie, D.; Vaca, S.; Carapito, C.; Chaoui, K.; Bruley, C.; Garin, J.; Cianferani, S.; Ferro, M.; Van Dorssaeler, A.; Burlet-Schiltz, O.; Schaeffer, C.; Coute, Y.; Gonzalez de Peredo, A. Benchmarking quantitative label-free LC-MS data processing workflows using a complex spiked proteomic standard dataset. *J. Proteomics* **2016,** *132*, 51-62.
(44) Cox, J.; Hein, M. Y.; Luber, C. A.; Paron, I.; Nagaraj, N.; Mann, M. Accurate proteome-wide label-free quantification by delayed normalization and maximal peptide ratio extraction, termed MaxLFQ. *Mol. Cell. Proteomics* **2014,** *13* (9), 2513-2526.
(45) Zhu, W. H.; Smith, J. W.; Huang, C. M. Mass spectrometry-based label-free quantitative proteomics. *J. Biomed. Biotechnol.* **2010**.
(46) Tirumalai, R. S.; Chan, K. C.; Prieto, D. A.; Issaq, H. J.; Conrads, T. P.; Veenstra, T. D. Characterization of the low molecular weight human serum proteome. *Mol. Cell. Proteomics* **2003,** *2* (10), 1096-1103.

(47) Geiger, T.; Wehner, A.; Schaab, C.; Cox, J.; Mann, M. Comparative proteomic analysis of eleven common cell lines reveals ubiquitous but varying expression of most proteins. *Mol. Cell. Proteomics* **2012,** *11* (3), M111 014050.
(48) Wilhelm, M.; Schlegl, J.; Hahne, H.; Gholami, A. M.; Lieberenz, M.; Savitski, M. M.; Ziegler, E.; Butzmann, L.; Gessulat, S.; Marx, H.; Mathieson, T.; Lemeer, S.; Schnatbaum, K.; Reimer, U.; Wenschuh, H.; Mollenhauer, M.; Slotta-Huspenina, J.; Boese, J.-H.; Bantscheff, M.; Gerstmair, A.; Faerber, F.; Kuster, B. Mass-spectrometry-based draft of the human proteome. *Nature* **2014,** *509* (7502), 582-587.
(49) Kim, M.-S.; Pinto, S. M.; Getnet, D.; Nirujogi, R. S.; Manda, S. S.; Chaerkady, R.; Madugundu, A. K.; Kelkar, D. S.; Isserlin, R.; Jain, S.; Thomas, J. K.; Muthusamy, B.; Leal-Rojas, P.; Kumar, P.; Sahasrabuddhe, N. A.; Balakrishnan, L.; Advani, J.; George, B.; Renuse, S.; Selvan, L. D. N.; Patil, A. H.; Nanjappa, V.; Radhakrishnan, A.; Prasad, S.; Subbannayya, T.; Raju, R.; Kumar, M.; Sreenivasamurthy, S. K.; Marimuthu, A.; Sathe, G. J.; Chavan, S.; Datta, K. K.; Subbannayya, Y.; Sahu, A.; Yelamanchi, S. D.; Jayaram, S.; Rajagopalan, P.; Sharma, J.; Murthy, K. R.; Syed, N.; Goel, R.; Khan, A. A.; Ahmad, S.; Dey, G.; Mudgal, K.; Chatterjee, A.; Huang, T.-C.; Zhong, J.; Wu, X.; Shaw, P. G.; Freed, D.; Zahari, M. S.; Mukherjee, K. K.; Shankar, S.; Mahadevan, A.; Lam, H.; Mitchell, C. J.; Shankar, S. K.; Satishchandra, P.; Schroeder, J. T.; Sirdeshmukh, R.; Maitra, A.; Leach, S. D.; Drake, C. G.; Halushka, M. K.; Prasad, T. S. K.; Hruban, R. H.; Kerr, C. L.; Bader, G. D.; Iacobuzio-Donahue, C. A.; Gowda, H.; Pandey, A. A draft map of the human proteome. *Nature* **2014,** *509* (7502), 575-581.
(50) The difficulty of a fair comparison. *Nat. Methods* **2015,** *12* (4), 273-273.
(51) Activated immunoaffinity supports. *Bio-Rad* **2019,** *http://www.biorad.com/webroot/web/pdf/lsr/literature/LIT156.pdf*.(accessed April 10, 2020)
(52) Saravis, C. A. Solid-phase radioimmunoelectrophresis: an assay for carcinoembryonic antigen. *J. Natl. Cancer Inst.* **1974,** *53* (4), 921-926.
(53) von Rechenberg, M.; Blake, B. K.; Ho, Y. S.; Zhen, Y.; Chepanoske, C. L.; Richardson, B. E.; Xu, N.; Kery, V. Ampicillin/penicillin-binding protein interactions as a model drug-target system to optimize affinity pull-down and mass spectrometric strategies for target and pathway identification. *Proteomics* **2005,** *5* (7), 1764-1773.
(54) Zhen, Y.; Xu, N.; Richardson, B.; Becklin, R.; Savage, J. R.; Blake, K.; Peltier, J. M. Development of an LC-MALDI method for the analysis of protein complexes. *J. Am. Soc. Mass. Spectrom.* **2004,** *15* (6), 803-822.
(55) Liu, W. J.; Bennett, A. L.; Ning, W. J.; Tan, H. Y.; Berwanger, J. D.; Zeng, X. Q.; Bruening, M. L. Monoclonal antibody capture and analysis using porous membranes containing immobilized peptide mimotopes. *Anal. Chem.* **2018,** *90* (20), 12161-12167.

For Table of Content Only: